JOURNAL OF MATERIALS SCIENCE 27 (1992) 6564–6572

Effect of tempering on development of carbide particles in 2.7Cr–0.6Mo–0.3V steel

J. JANOVEC, A. VÝROSTKOVÁ
Slovak Academy of Sciences, Institute of Experimental Metallurgy, Watsonova 47, 04353 Košice, Czechoslovakia

A. HOLÝ
Welding Research Institute, Bratislava, Czechoslovakia

To study the influence of tempering conditions (823–1058 K, 9–3600 ks) on the phase transformations and changes of morphology, size and chemical composition of carbide particles in 2.7Cr–0.6Mo–0.3V steel, the methods of, electron diffraction and EDXS/STEM have been used. Three carbide types: M_3C, M_7C_3 and MC have been identified altogether, the last two of which are equilibrium ones under given conditions. Diagrams describing changes in chemical composition of carbide particles and the average size during tempering have been constructed. In the development of carbide chemical composition three stages have been recorded. The carbide particles grow continuously with the increasing of time and/or temperature of tempering.

1. Introduction

Low-alloyed steels are widely used in the production of steam and nuclear power generation plants. Typical components include pressure vessels, bolts, turbine casings, rotor forgings etc. [1, 2]. The components are working at elevated temperatures and this must be taken into account in their material design. From this point of view a ferrite–carbide microstructure of the tempered state is considered as optimum [2, 3]. Carbide particles play an important role in such microstructure, and their influence on mechanical properties is generally known [4, 5].

The processes of structure development during production and the structure changes during exploration depend on many internal and external factors. The bulk chemical composition is the main internal factor influencing the structure, chemical composition and stability of carbide particles [3, 6–9]. The influence of the chemical composition of Cr–Mo–V steels on the structural stability of carbide particles during tempering at 973 K for 3600 ks is evident from the constitutional diagram in Fig. 1 [6]. The letter M represents a comprehensive metallic component in a carbide formula. The influence of the chemical composition of low-alloyed Cr–Mo and Cr–Mo–V steels on the lattice parameter a and chemical composition of M_2C carbide is schematically documented in Fig. 2 [8]. The course of the relationships presented in Fig. 2 shows that increasing the Cr/Mo value (wt % ratio) increases the relative substitution of Cr in M_2C carbide and decreases the lattice parameter a. The effect of heat and therefore deformation on structure development is one of the most important external factors. In conditions of isothermal exposure the state of steels is characterized by the Larsen–Miller parameter P:

$$P = T(19.77 + \log t) \times 10^{-3}$$

The above-mentioned temperature T(K) and holding time t(ks) have an essential influence on the structural stability of carbide phases (Fig. 3) [10]. The influence of deformation on the carbide phase changes has been studied (e.g. [2, 11]). Wang Zhong-Guang *et al.* [2] showed in the 0.3C–1.2Mo–0.2V (wt %) steel that a coarsening of longitudinal carbide particles and relative increase of Mo and V contents in these particles occur as a result of cyclic deformation at ambient temperature.

The methods of carbide particle study have undergone an essential development as well. The originally dominant methods of electrochemical detaching and X-ray diffraction [12–14] have been replaced by procedures of electron microscopy (ELMI) and recently subjoined with the microanalytical methods of energy-dispersive X-ray spectroscopy (EDXS) with scanning transmission electron microscopy (STEM) [15–17].

The aim of the work is to judge the influence of tempering conditions on carbide particle stability in the 2.7Cr–0.6Mo–0.3V steel, and in parallel to quantify the changes in chemical composition and size of carbide particles during isothermal transition of the steel from the quenched to the equilibrium state.

2. Experimental procedure

The heat treatment of the experimental steel (Table I) consisted of

0022–2461

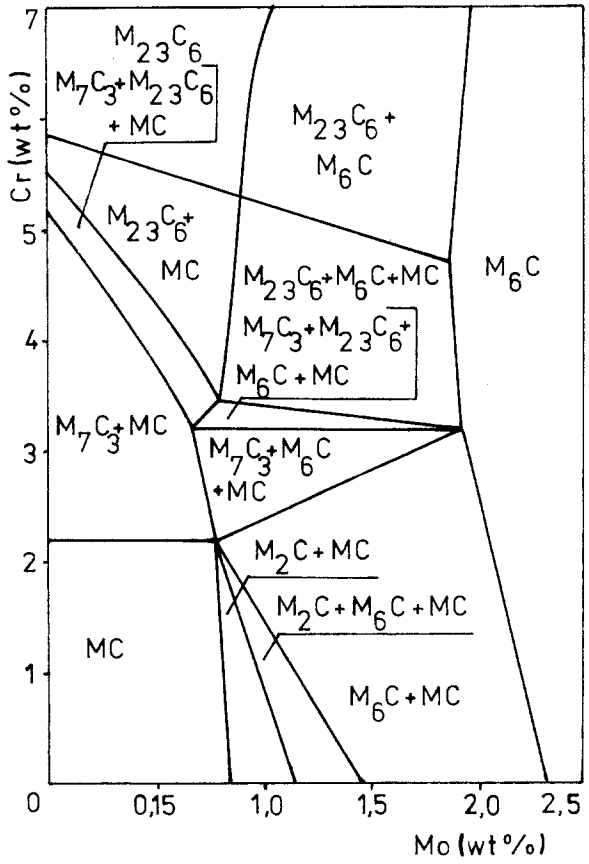

Figure 1 Constitutional diagram for low-alloyed Cr–Mo–V steel with constant V content (0.5 wt %). Tempering conditions: 973 K, 3600 ks. The phase stability of carbides is expressed as a function of Cr and Mo content [6].

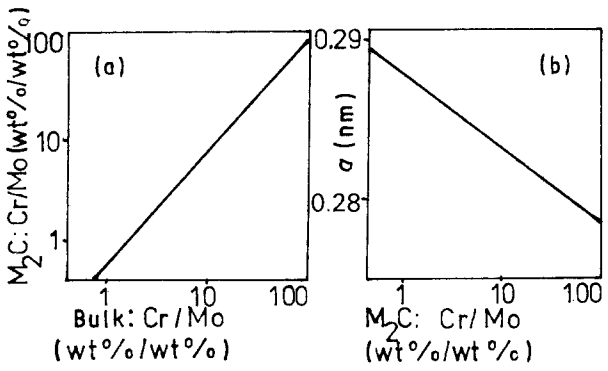

Figure 2 Schematic dependences [8]: (a) M_2C carbide chemical composition expressed by Cr/Mo ratio against the bulk chemical composition of Cr–Mo–V low-alloyed steels, (b) lattice parameter *a* as a function of Cr/Mo ratio for carbide M_2C.

(i) first austenitization at 1423 K for 3.6 ks with oil quenching;

(ii) second austenitization at 1163 K for 7.2 ks with oil quenching;

(iii) tempering at five different temperatures and times in the interval 823–1058 K for 9–3600 ks.

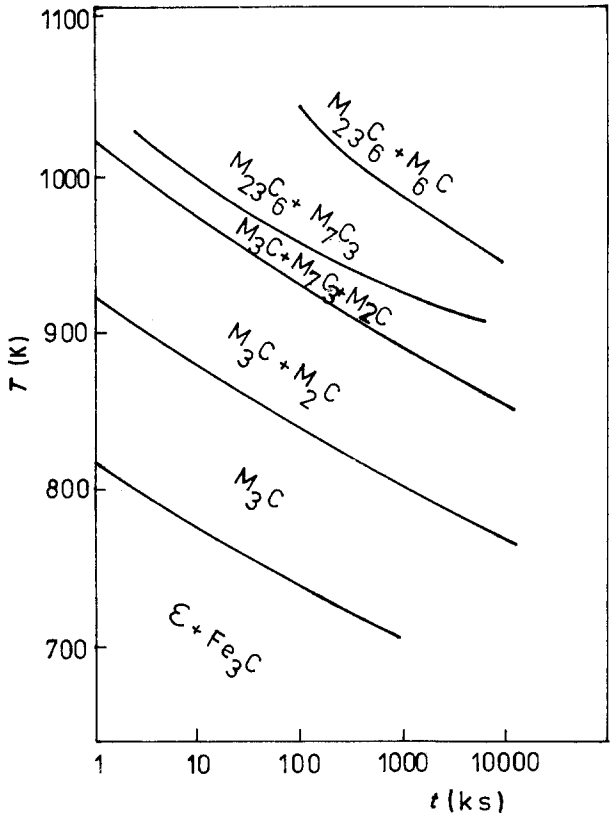

Figure 3 Carbide phase stability diagram for 2.25Cr–1Mo steel [10]. Tempering conditions: 700–1050K, 1–10000 ks.

During the heat treatment, prismatic samples 10 mm × 10 mm × 25 mm were placed in capsules made of quartz. After the completed heat treatment a surface layer of about 1 mm width was removed from the samples. The hardness H_v (294 N) and microstructure of all states were measured and evaluated, respectively. A solution of 1 vol. part HNO_3 and 49 vol. parts CH_3OH was used to reveal microstructure. Carbide particles extracted into the carbon replicas (in electrolyte $HClO_4$:CH_3COOH = 1:20, $T = 295$ K, $U = 20$ V, $i = 1.6$ mA mm^{-2}) were submitted to the ELMI analyses. These consisted (Fig. 4) of:

(i) evaluation of the morphology and size of carbide particles (Fig. 4a),

(ii) crystallographic identification of carbide by means of point electron diffraction patterns (Fig. 4c), and

(iii) chemical composition identification of carbide metallic component by EDXS/STEM (Fig. 4b).

In 26 different states, one quenched (N) and 25 tempered (Table II) the number of carbide particles analysed was 358. The analyses were realized on a STEM JEM 2000 CX and an analytical unit EDAX 9900. The average carbide particle size was measured on the carbide extraction replicas by the method described

TABLE I Chemical composition of experimental steel

Element	C	Si	Mn	Cr	Mo	V	Ni	Al	P	N
(wt %)	0.14	0.23	0.44	2.70	0.59	0.32	0.14	0.008	0.014	0.005
(at %)	0.65	0.46	0.45	2.89	0.34	0.35	0.13	0.018	0.027	0.019

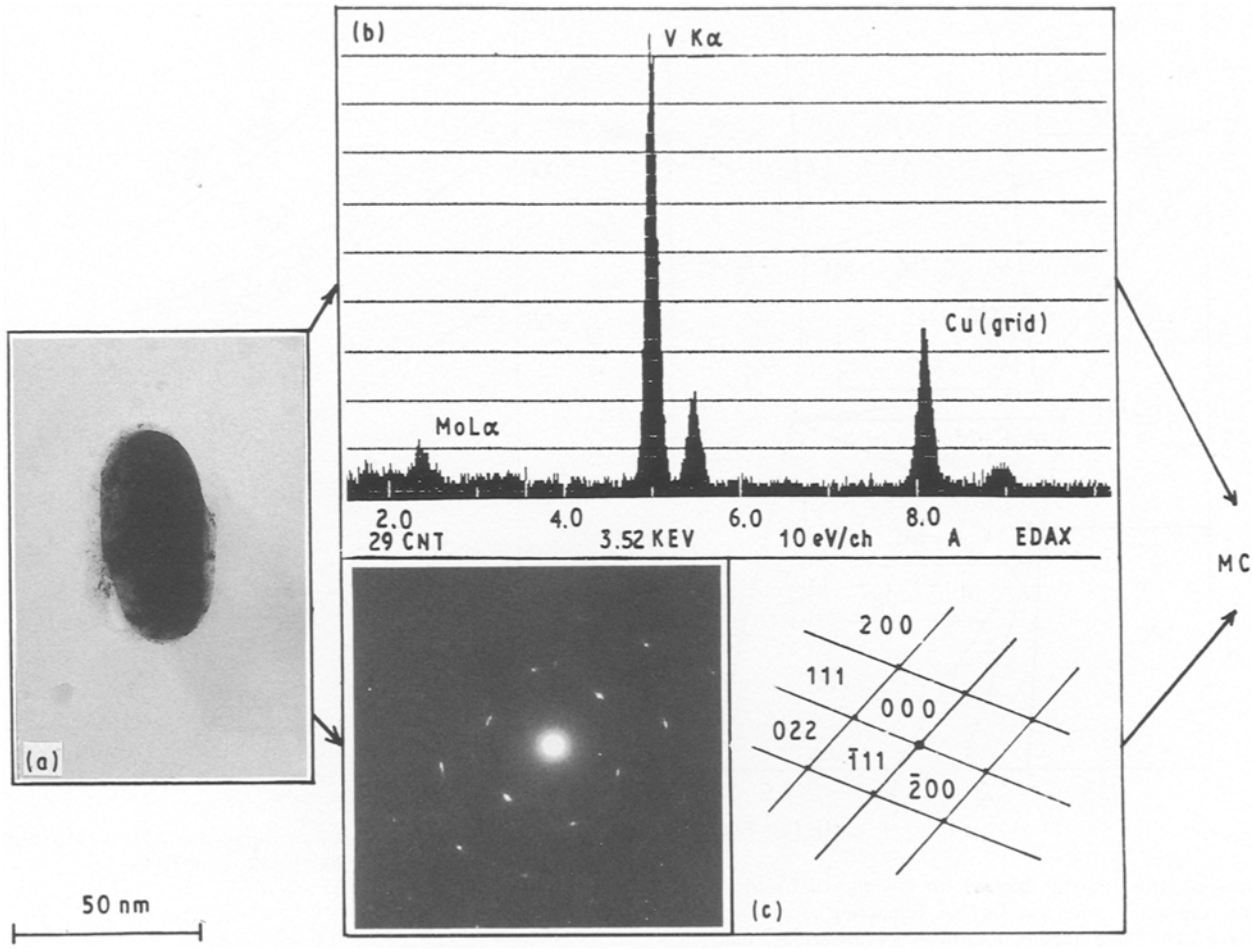

Figure 4 Procedure used for carbide particle identification: (a) TEM documentation of particles, (b) EDX spectrum, (c) electron diffraction pattern.

TABLE II Heat treatment and Larsen–Miller parameter of experimental states

Tempering temperature (K)	Time of tempering (ks)				
	9	54	360	1080	3600
823	16.8	17.4	18.1	18.6	18.9
893	18.2	18.9	19.7	20.1	20.5
938	19.1	19.9	20.6	21.1	21.6
1023	20.9	21.7	22.5	22.9	23.5
1058	21.7	22.6	23.3	23.8	24.6

by Purmenský *et al.* [18]. The point electron diffraction patterns and EDX spectra were computerized. A personal computer was also used to assess the results, for instance by the construction of three-dimensional diagrams: tempering temperature–time of tempering–chemical composition (size) of carbide.

3. Results

The chemical analysis of the steel is given in Table I. Analysed element concentrations are expressed in both weight and atomic percentage. The relationships between hardness and tempering temperature for five tempering time are documented on Fig. 5. The relationships presented have a decreasing course over the whole range.

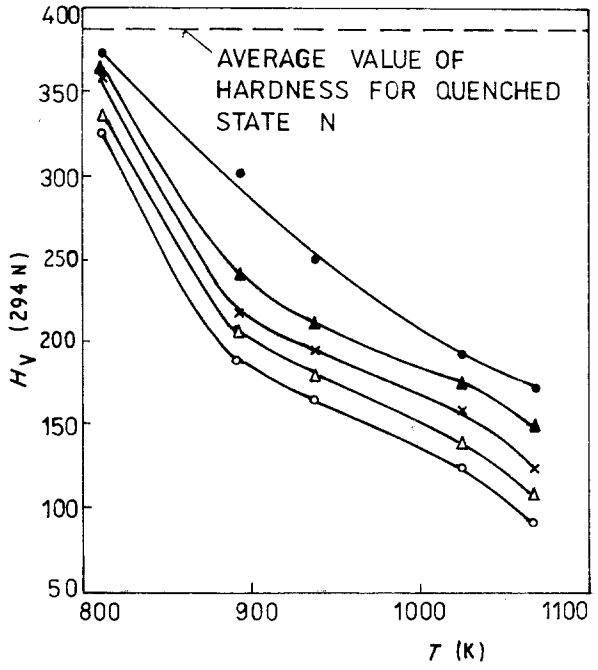

Figure 5 Dependence of hardness H_v (294 N) on tempering temperature for various tempering times: (●) 9 ks, (▲) 54 ks, (×) 360 ks, (△) 1080 ks, (○) 3600 ks.

The microstructures of chosen experimental states are documented on Fig. 6. The quenched state N (Fig. 6a) consists of products of non-equilibrium austenite decomposition, largely those of needle-shaped

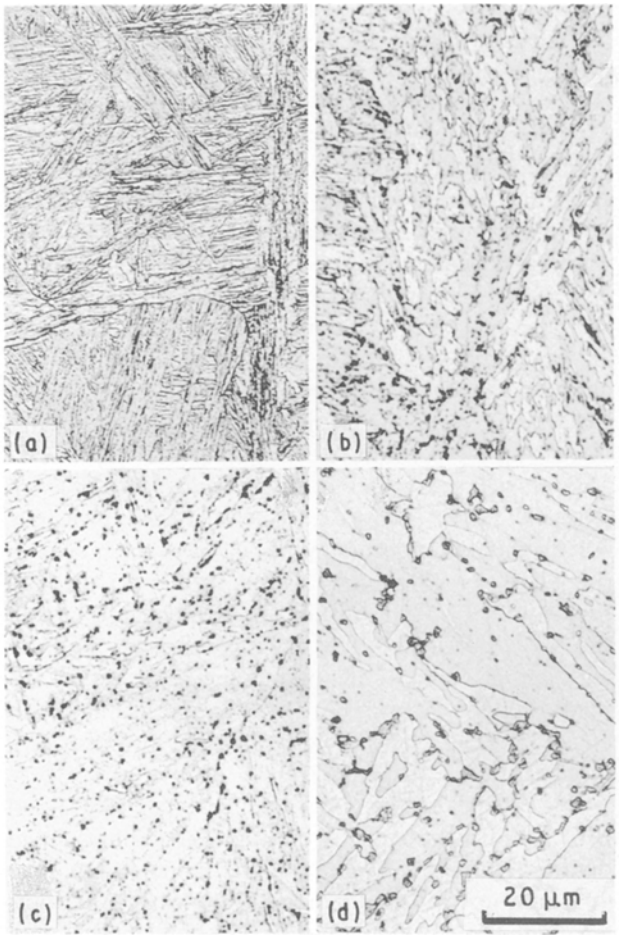

Figure 6 Microstructure changes as a consequence of various tempering conditions: (a) quenched state N, (b) 823 K for 360 ks, (c) 893 K for 54 ks, (d) 1058 K for 360 ks.

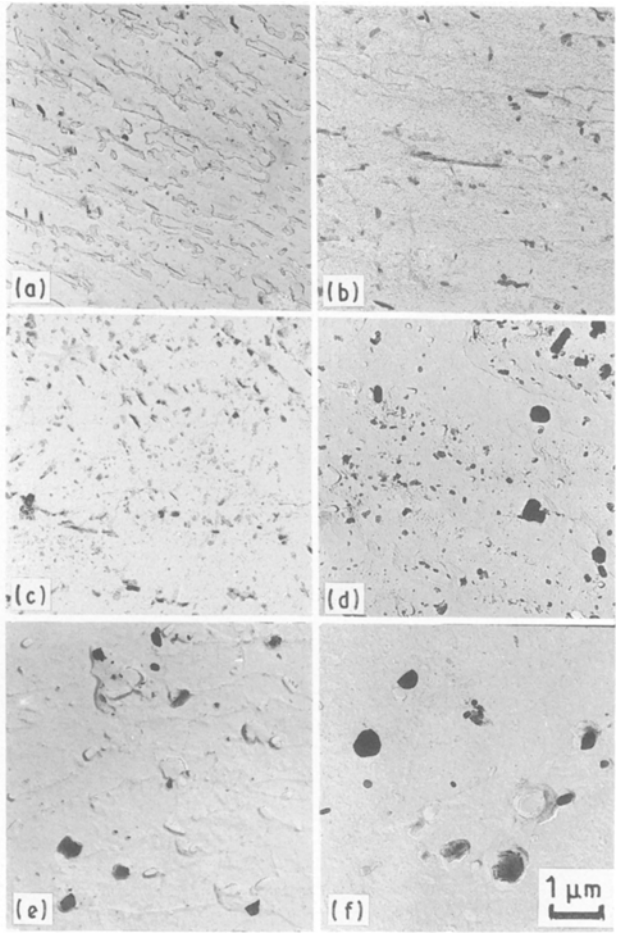

Figure 7 Changes in morphology, size and density of carbide particles after tempering: (a) quenched state N, (b) 823 K for 360 ks, (c) 893 K for 9 ks, (d) 893 K for 3600 ks, (e) 938 K for 1080 ks, (f) 1058 K for 360 ks.

morphology. This morphology is also preserved during low-temperature tempering (Fig. 6b). At higher tempering temperatures the needle-like character decreases and individual structure parts are evidently coarsened (Fig. 6c and d), which becomes strikingly evident at carbide particles (Fig. 6d). The carbide particle coarsening with increasing temperature and time of tempering can also be seen in the photos in Fig. 7. The figures represent carbide particles extracted into the carbide replicas. From the morphology point of view, the particles can be divided into longitudinal (angular, oval) and globular. The former represent usually M_3C and M_7C_3 carbide types. They occur mainly in low-tempered states. The latter are mostly MC and some of the M_7C_3 carbide types (above all in higher-tempered states).

The results of carbide identification in tempered states are documented in Fig. 8. In the structure of the quenched state N, carbide particles of M_3C and MC types have been identified. MC carbide also kept its structural stability during subsequent tempering while the carbide M_3C showed itself as an unstable one, and at values of parameter $P > 19.1$ (Table II, Fig. 8) it was fully substituted by M_7C_3 carbide. Three areas specified by experimentally measured points within the framework of the carbide phase stability diagram can be distinguished. Each point represents the carbide identification results of one of the experimental states.

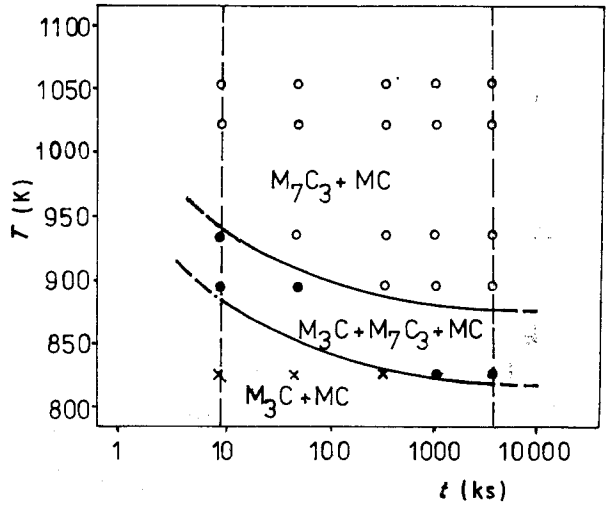

Figure 8 Carbide phase stability diagram for 2.7Cr–0.6Mo–0.3V steel, 823–1058 K and 9–3600 ks.

There is an area of stable M_3C and MC carbide existence in the low-temperature part of the diagram. As many as 68% of the experimental points fill in the high-temperature area consisting of M_7C_3 + MC carbide phases. Between the above-mentioned areas lies a

narrow transition band of the coexistence of three carbides: M_3C, M_7C_3 and MC.

Four elements, namely Fe, Cr (dominant) and V, Mo (minor), have been found by the EDXS/STEM method in the metallic component of M_3C and M_7C_3 carbides. The results of quantitative analysis of EDX spectra have been used to evaluate the average value of the ratio of dominant elements (Cr/Fe for M_7C_3 carbide and Fe/Cr for M_3C carbide), the ratio of minor elements (V/Mo) and the ratio of the dominant and minor element sums. In the metallic component of MC carbide only two elements have been identified: dominant V and minor Mo. Therefore only the V/Mo ratio has been stated for this carbide type. All the above-mentioned ratios have been determined from the weight percentage concentrations.

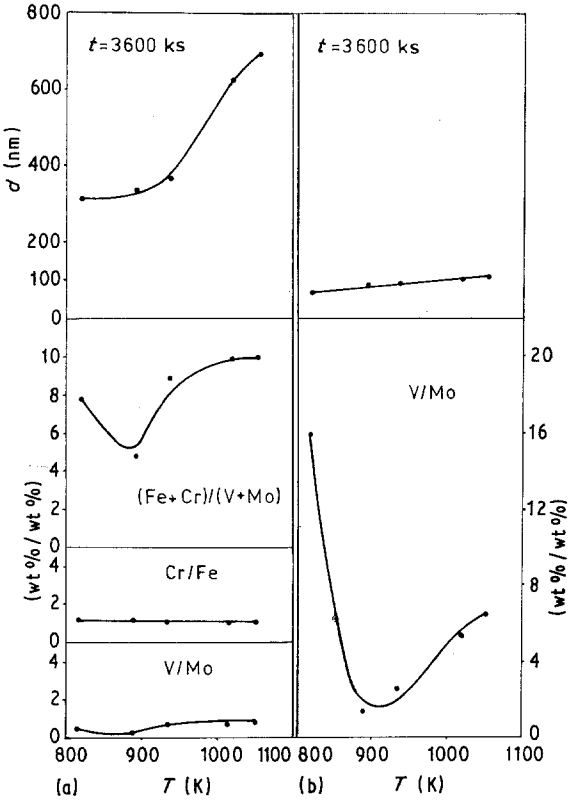

Figure 9 Influence of tempering temperature on the average size and chemical composition of carbide particles after 3600 ks: (a) M_7C_3 carbide, (b) MC carbide.

The average values of analysed particle size d and the ratios of element contents in the metallic component of carbides after an exposure time 3600 ks at chosen temperatures are documented on Fig. 9. Fig. 9a represents the results for M_7C_3 carbide. With increasing temperature of tempering the size of carbide particles increases at first slightly and later intensively; the Cr/Fe ratio does not change in principle. A local minimum occurs in the course of the functions $(Fe + Cr)/(V + Mo) = f(T)$ and $V/Mo = f(T)$ at temperature 893 K. The results for MC carbide are in Fig. 9b. While the particle size increases continuously with an increase of tempering temperature, in the relationship $V/Mo = f(T)$ there is a continuous decrease of V/Mo values, finished by the presence of a local minimum at temperature 893 K.

The kinetics of the changes in carbides M_7C_3 and MC can be evaluated from the three-dimensional diagrams in Figs 10 and 11. With increasing time and/or temperature of tempering the carbide particle size continuously increases too. This tendency is more accentuated for M_7C_3 carbide (Fig. 10b) and manifests itself above all during the high-temperature tempering. Changes in chemical composition of MC carbide, expressed by means of the V/Mo ratio, are documented on Fig. 11a. The figure shows a trough between the points [893 K, 3600 ks] and [1058 K, 9 ks] going through the areas with P parameter values

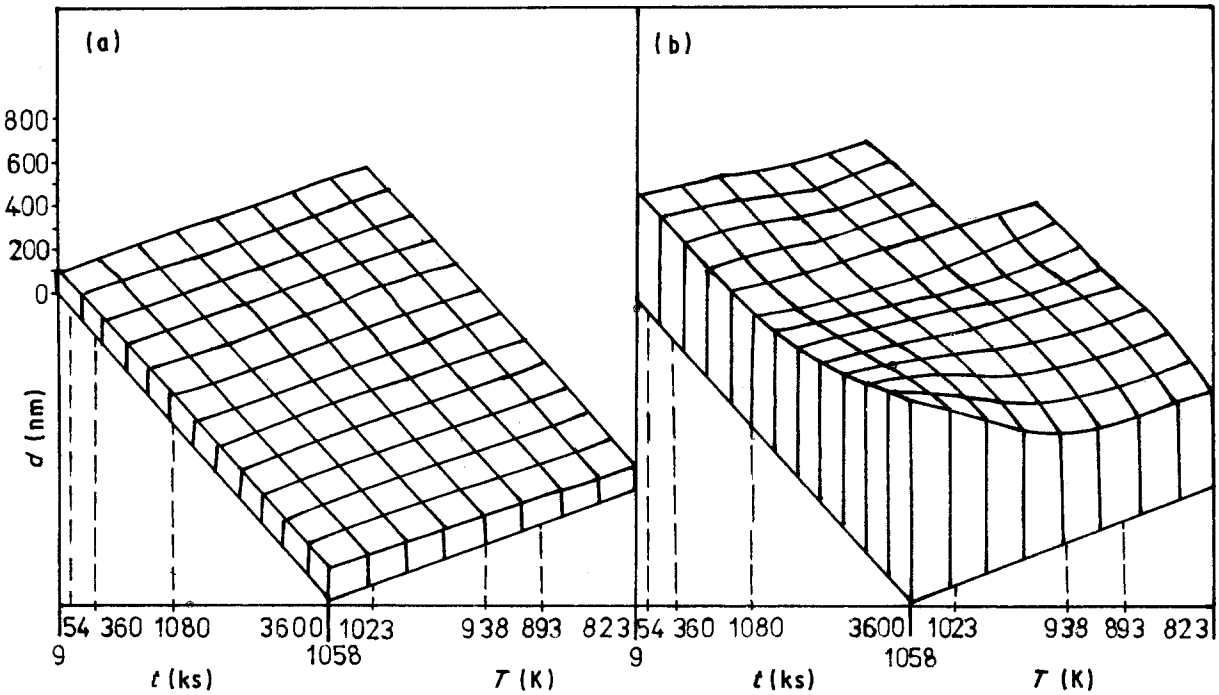

Figure 10 Influence of tempering time and temperature (three-dimensional diagram) on the average size of carbide particles: (a) MC carbide, (b) M_7C_3carbide.

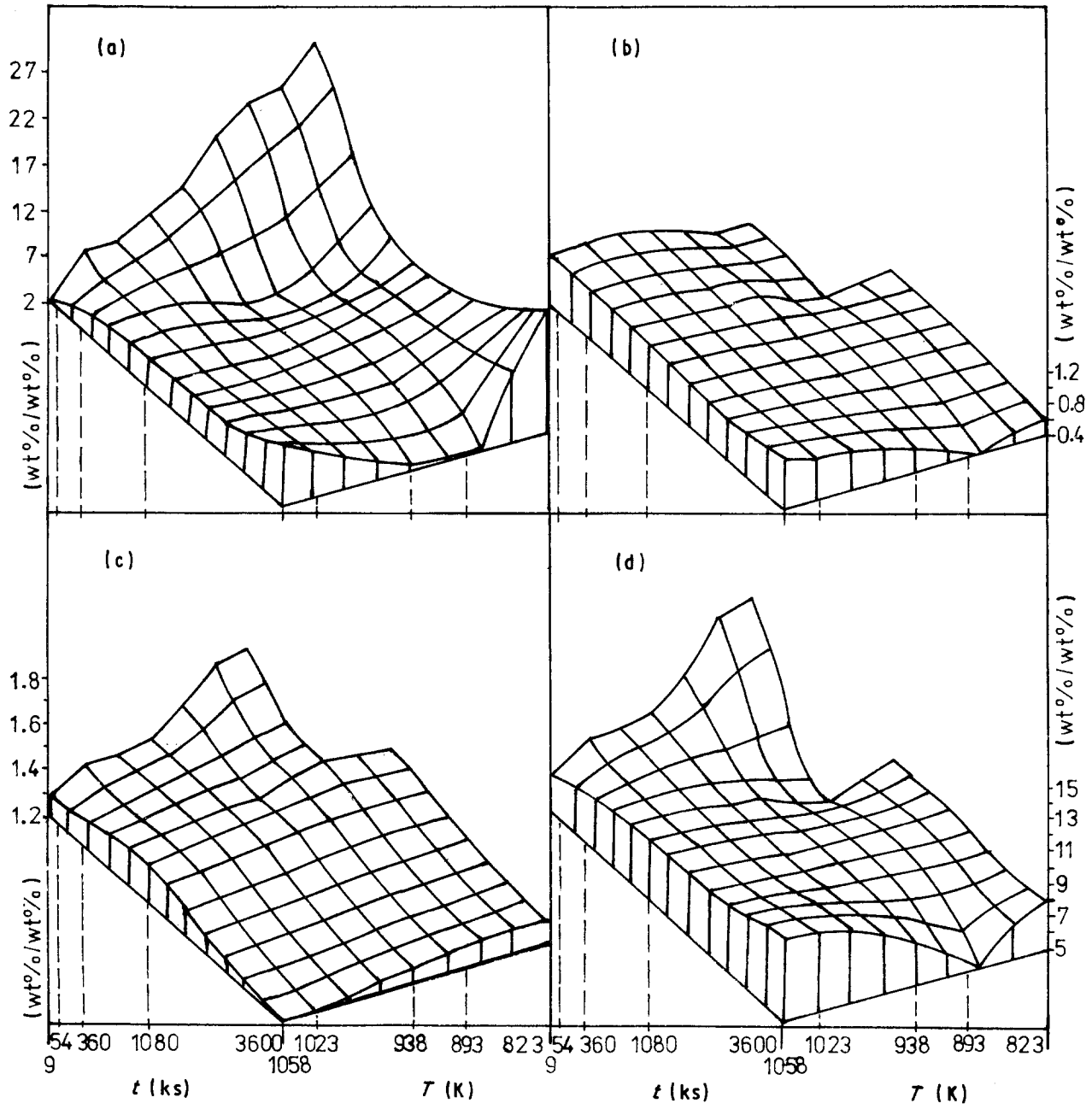

Figure 11 Influence of tempering time and temperature (three-dimensional diagram) on the average chemical composition of the metallic component in carbide phases: (a) MC V/Mo, (b) M_7C_3 V/Mo, (c) M_7C_3 Cr/Fe, (d) M_7C_3 (Cr + Fe)/(V + Mo).

$P = 21 \pm 0.5$. The trough forms natural bounds between lower- and higher-tempered states. For the former state it holds, that with increasing temperature and time of tempering the ratio V/Mo decreases. In the latter state the converse occurs. A similar course can be seen in the relationship (Cr + Fe)/(V + Mo) = $f(T, t)$ constructed for M_7C_3 carbide (Fig. 11d). The changes in relative substitution of minor alloying elements Mo and V in M_7C_3 carbide are documented in Fig. 11b. They achieve minimal values at 893 K, as evidenced by the presence of a trough in the three-dimensional diagram. For the dominant alloying elements in M_7C_3 a continuous decrease of Cr/Fe value with increasing temperature and time of tempering has been noticed.

ELMI analysis of carbide particles in the quenched state N gave the following results. For MC: $d = 35$ nm, V/Mo = 30.0 wt %/wt %; for M_3C: $d = 100$ nm, V/Mo = 0.9 wt %/wt %, Fe/Cr = 18.0 wt %/wt %, (Cr + Fe)/(V + Mo) = 20.0 wt %/wt %. Besides the state N, M_3C carbide has been identified also in the next eight tempered states. In the relationships of Fig. 12 documenting the size and chemical composition changes of M_3C carbide with tempering time, there are differently marked experimental points for individual tempering temperatures. From the course of these relationships it is evident that with increasing time and temperature of tempering there are increases of Cr relative to Fe and Mo relative to V content, and also of minor alloying elements compared with dominant ones. The particles of carbide M_3C enlarge simultaneously.

4. Discussion

4.1. Changes of carbide stability

Tempering is, from the thermodynamical point of

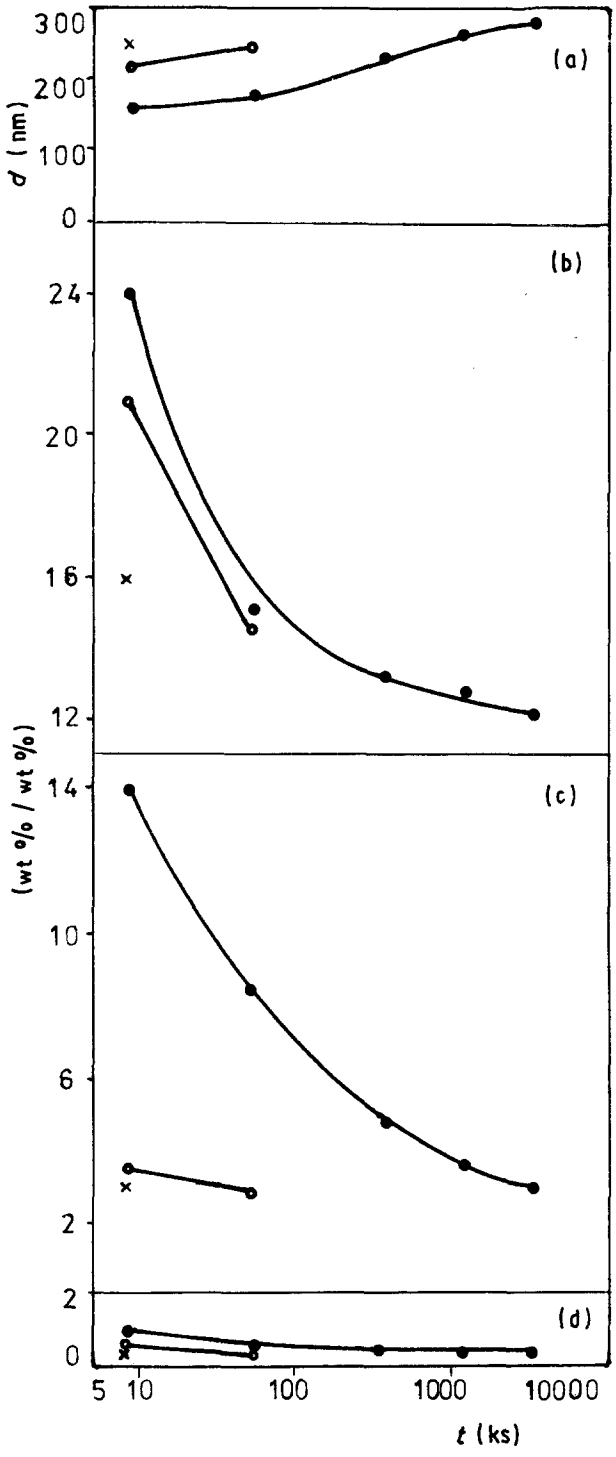

Figure 12 Influence of tempering time and temperature on the average size of M_3C carbide: (a) d; (b) (Fe + Cr)/(V + Mo) for (●) 823 K, (○) 893 K, (×) 938 K; (c) Fe/Cr; (d) V/Mo.

view, an irreversible process, during which a system (the experimental steel) reaches a more stable, so-called stationary state. This used to be denoted in materials science as an equilibrium one [12]. In accordance with Andrews *et al.* [6] (Fig. 1), Smith [19] (Woodhead and Quarrell [20]), Čadek [21] and others it was confirmed that in the experimental steel, ferrite and the carbides M_7C_3 and MC belong among the equilibrium phases. The transition of the system to the equilibrium state at P values equal to 19.0 was noted, which is in good accord with the results published by Andrews *et al.* [6]. The absence of M_2C, M_6C and $M_{23}C_6$ carbides in the microstructure of the analysed states is conditioned by the chemical composition of the steel. From papers dealing with the stability of carbides in low-alloyed steels [6, 7, 21, 22] it follows that in order to achieve the stability of the above-mentioned carbides, for instance a decrease of C level and an increase of Mo level in the steel would be needed. The time–temperature conditions for nucleation of the first-originating MC carbides could not be evaluated because of the above-mentioned presence of carbide in the quenched state N. According to Andrews *et al.* [6], MC initiation can be expected at values of $P = 18$ which in experimental conditions corresponds to the lowest tempering temperature of 823 K.

4.2. Changes in carbide chemical composition

The development of the chemical composition of carbide phases during tempering has been accomplished in three stages. Each stage is characterized by starting and final states from the point of view of carbide types and their chemical composition.

4.2.1. The first stage

The quenched state N (Figs 6a and 7a) is an initial one in the first stage. Its structure consists of a solid solution with a relatively high content of C and carbide-forming alloying elements Cr, V, Mo and with carbide particles of $[Fe(Cr, Mo, V)]_3C$ and [V(Mo)]C types. The metallic component in the formulae is written in a way that enables one to differentiate the dominant alloying elements from the minor ones (in parentheses). The final state is represented by a ferrite–carbide microstructure with $[Fe, Cr(Mo, V)]_3C$ and [V(Mo)]C carbide types. What is the mechanism of the transition from the initial to the final state? During the heating of the initial state at the tempering temperature, there are gradients of chemical potentials of the elements C, Cr, Mo and V between carbide phases and the solid solution. The experimental results (Figs. 11 and 12) show that in the first stage the potential differences of C, Cr (in relation to M_3C carbide), V (predominantly in relation to MC carbide) and partly Mo (in relation to both M_3C and MC carbides) are reduced, as manifested itself in the coarsening and increasing volume portion of carbide particles. As a result, there are increases of Cr (from 7 to 23%, Fig. 12c) and Mo + V (from 4 to 8%, Fig. 12b) contents in M_3C carbide. The relative content to Mo in carbides during the first stage is minimal. This can be ascribed to the lower affinity of Mo for C (in comparison with Cr and V), but also to the fact that Mo in the experimental steel does not form its own special carbide. Examination of the changes in carbide composition during the first stage is most suitably done in the states tempered at 823 K, because at this temperature they are taking place more slowly than at higher temperatures. For Cr, from a comparison of Figs 8 and 12c it follows that to alloy the carbide M_3C is thermodynamically more advantageous than to form its own Cr carbide. M_7C_3 particle

nucleation occurs only after Cr saturation in the M_3C carbide (Fig 12b), and they are probably located around M_3C particles, manifesting themselves at places of increased Cr content [3].

4.2.2. The second stage

It is evident that the initial state of the second stage is identical with the final state of the first stage. The second-stage final state consists of a ferrite–carbide microstructure with [Cr, Fe(Mo, V)]$_7C_3$ and [V, Mo]C carbides. During the second stage two main processes occur simultaneously:

(i) The loss of [Fe, Cr(Mo, V)]$_3C$ carbide structure stability and its full replacement by the carbide [Cr, Fe(Mo, V)]$_7C_3$. The ratio of dominant alloying elements in the new carbide is very stable and changes minimally with time and temperature of tempering (Figs 9a and 11c).

(ii) The Mo content increases in both M_7C_3 and MC equilibrium carbides, probably as a consequence of the increasing chemical activity of this element in carbide phases. The reason for higher Mo chemical activity (mainly in MC carbides) is an effort to balance the chemical potentials of this element in all phases of the system. Mo is the only carbide-forming element whose distribution between the solid solution and carbide phases is, in the second stage, far from the equilibrium state. Since Mo in the experimental steel does not form its own carbide, it has a tendency to alloy the existing stable carbides M_7C_3 and MC. Because the relationships V/Mo $= f(T)$ for carbide MC, (Fe + C)/(V + Mo) $= f(T)$ and V/Mo $= f(T)$ for carbide M_7C_3 in Fig. 9 achieve a minimum at 893 K (i.e. the relative Mo content in carbides has the highest value), one can assume that after 3600 ks exposure at this tempering temperature the system is still in the second stage.

4.2.3. The third stage

This stage concerns carbide development in the stationary state. The chemical composition of the carbides is stable enough to hold the same schematic formulae for both initial and final states: [Cr, Fe(Mo, V)]$_7C_3$ and [V, Mo]C. After the balancing of Mo chemical potentials in the second stage the system is in equilibrium. It is probable that in such a situation the higher affinity of V and Cr for C will again dominate, which can lead to a slight decrease of Mo content in both equilibrium carbides.

4.2.4. General description

The development of the chemical composition of carbide during tempering cannot be described generally without considering the fact that tempering is an isothermal process, in the framework of which the time of tempering is the only independent variable. The experimental results confirm the assumption of a time shift of Mo chemical activity maximum in relation to Cr and V, which manifests itself by the presence of troughs in the relationships in Figs 9 and 11. This time shift is temperature-dependent. That is why the system need not achieve at lower tempering temperatures even the second stage, while at high temperatures it already achieves the third stage after a very short period. This idea is graphically interpreted by means of the diagram in Fig. 13. The ratio M/Mo is the dependent variable (M = V, or Cr, or V + Cr), t_x is the time coordinate of the local minimum in the relationship M/Mo $= f(t)$, and $t_0 - t_n$ and $T_1 - T_4$ are the tempering time and temperatures, respectively. Fig. 13 explains the course of the relationships in Figs 9 and 11 and also the origin of the troughs.

4.3. Changes of morphology and size of carbide particles

From the morphological viewpoint the development of carbide particles during tempering can be divided into three stages:

(a) spheroidization of originally elongated carbide particles present in the microstructure of the initial quenched state;

(b) slow growth of spheroidized carbide particles; and

(c) fast growth of these particles.

For the carbide M_3C only the first two and for M_7C_3 the last two stages have been observed. At lower tempering temperatures the particle growth rate of both equilibrium carbides is similar; at higher temperatures the carbide MC maintains its former slow rate, while M_7C_3 carbide moves into the stage of fast growth. This phenomenon has been described and analysed in a number of works (e.g. [20, 23]). The faster growth of M_7C_3 carbide particles is a result of

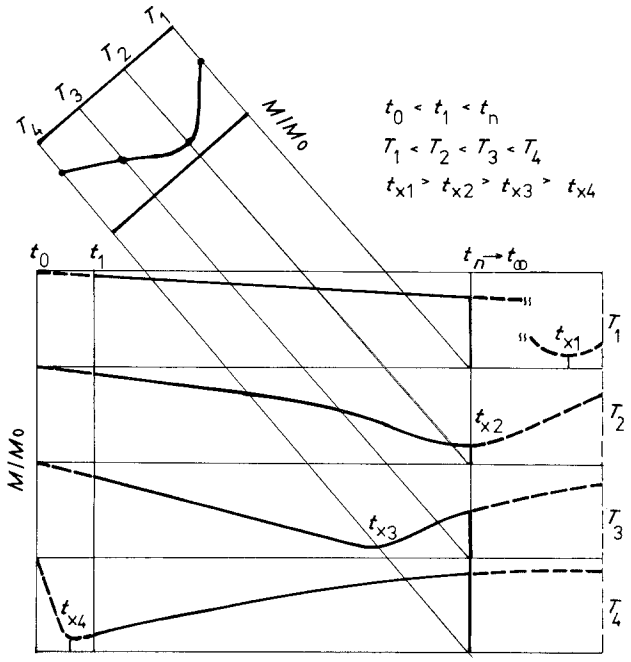

Figure 13 Schematic diagram explaining the influence of tempering conditions on the changes of carbide phase chemical composition expressed by the M/Mo ratio where M = V, Cr or V + Cr.

the lower activation energy of particle coarsening and chemical bond strength [18]. In addition, the Cr diffusivity in ferrite is higher in comparison with that of V [24]. The courses of the relationships H_v (294 N) $= f(T)$ (Fig. 5) and $d = f(T, t)$ (Fig. 10) show that during the tempering of the experimental steel, secondary hardening as a consequence of secondary precipitation of fine carbide particles did not occur. That is why particle growth in the stationary state can be considered as a continual process that proceeds without the disturbance of additional phase transformations.

5. Conclusions

The results of phase transformation and changes in morphology, size and chemical composition of carbide particles in 2.7Cr–0.6Mo–0.3V steel during tempering conditions 823–1058 K and 9–3600 ks can be summarized as follows:

1. For the experimental steel the M_7C_3 and MC carbide types are equilibrium ones.
2. In the metallic component of MC carbide two elements, V and Mo, have been found while in M_3C and M_7C_3 four elements have been found, Fe and Cr as dominant (90 wt %) and V and Mo as minor ones.
3. The MC carbide is stable over the whole temperature range. An intensive alloying of M_3C carbide with Cr precedes the nucleation of further equilibrium carbide M_7C_3.
4. In M_7C_3 carbide the Cr/Fe ratio is stable, but V/Mo and (Fe + Cr)/(V + Mo) ratios are changed in relation to the time–temperature conditions of tempering. Similar changes have also been found in the carbide MC (ratio V/Mo).
5. Troughs in the temperature and time–temperature relations of the ratios V/Mo (for MC and M_7C_3 carbides) and (Fe + Cr)/(V + Mo) (for M_7C_3 carbide) have been found.
6. It has been confirmed that with increased time and/or temperature of tempering the sizes of carbide particles of M_3C, M_7C_3 and MC types grow continuously.

References

1. G. L. DUNLOP and R. W. K. HONEYCOMBE, *Met. Sci.* (April 1976) 124.
2. WANG ZHONG-GUANG, K. RAHKA, P. NENONEN and C. LAIRD, *Acta Metall.* **33** (1985) 2129.
3. J. A. SENIOR, *Mater. Sci. Engng.* **A103** (1988) 263.
4. S. A. PARSONS and D. V. EDMONDS, *Met. Sci. Technol.* **3** (1987) 894.
5. K. ASAKURA, A. KOHYAMA and T. YAMADA, *ISIJ Int.* **30** (1990) 947.
6. K. W. ANDREWS, H. HUGHES and D. J. DYSON, *JISI* **210** (1972) 337.
7. J. PILLING and N. RIDLEY, *Met. Trans.* **13A** (1982) 557.
8. R. PETRI, E. SCHNABEL and P. SCHWAAB, *Arch. Eissenhuttenwes.* **52** (1981) 71.
9. J. JANOVEC, A. GÜTH, A. VÝROSTKOVÁ and B. ŠTEFAN, *Kovové Materiály* **26** (1988) 714.
10. R. G. BAKER and J. NUTTING, *JISI* **192** (1959) 257.
11. R. D. K. MISRA and T. V. BALASYBRAMANIAN, *Acta Metall.* **38** (1990) 1263.
12. K. W. ANDREWS and H. HUGHES, *Iron Steel* **31** (1958) 43.
13. J. ČADEK, R. FREIWILLIG and O. DUPAL, *Hutnické Listy* **16** (1961) 874.
14. K. KUO, *JISI* **184** (1956) 258.
15. F. JANDOŠ, R. RIMAN and A. GEMPERLE, "Využiti Modernich Laboratornich Metod v Metalografii" (SNTL, Praha, 1985).
16. A. GÜTH, L. KAUN, A. KOTHE, D. MULLER and J. RICHTER, *Scripta Metall.* **21** (1987) 163.
17. S. KARAGÖZ, I. LIEM, E. BISCHOFF and H. F. FISCHMEISTER, *Met. Trans.* **20A** (1989) 2695.
18. J. PURMENSKÝ, V. FOLDYNA, B. MILLION and J. VŘEŠŤAŁ *Kovové Materiály* **18** (1980) 171.
19. R. SMITH, Special Report No. 64 (1959) p. 307.
20. J. H. WOODHEAD and A. G. QUARRELL, *JISI* **203** (1965) 605.
21. J. ČADEK, O. DUPAL and R. FREIWILLIG, *Hutnické Listy* **17** (1962) 573.
22. J. YU and C. J. McMAHON Jr, *Met. Trans.* **11A** (1980) 277.
23. T. MUKHERJEE, and B. R. NIJHAVAN, *JISI* **207** (1969) 621.
24. H. OIKAWA, *Tech. Rep. Tohoku Univ.* **27** (1982) 215.

Received 28 June 1991
and accepted 7 February 1992